

# Design of a Wide Planar Waveguide Antenna for UHF Near-Field RFID Reader With High Reading Rate

Yusuke Ozawa, Qiang Chen<sup>ID</sup>, Senior Member, IEEE, Kunio Sawaya<sup>ID</sup>, Life Fellow, IEEE, Machiko Oouchida, and Masatomo Tokieda

**Abstract**—UHF near-field RFID reader antenna based on leaky waveguide is proposed and the performance is evaluated using numerical simulation and experiment. In order to suppress the standing wave along transverse direction, a pair of notches is placed on the transverse edge of the mesh layer of the planar waveguide. Diversity operation by switching impedance of the end terminal of the planar waveguide antenna is also introduced to suppress the standing wave effect along longitudinal direction. Numerical simulation and experiment show that the near-field null lines parallel to the longitudinal direction is almost removed by the presence of the notches and the distribution of the field strength becomes almost uniform because of the utilization of the switching diversity. It is demonstrated that the reading performance of the commercial RFID tags is greatly improved by using the proposed RFID reader antenna with the diversity operation of termination impedance.

**Index Terms**—Planar waveguide antenna, reader antenna, UHF RFID, switching diversity.

## I. INTRODUCTION

**A** RADIO frequency identification (RFID) technology is capable of tracking and identifying items via communications between RFID tags attached to the items and a reader antenna. Simultaneous detectability of RFID tags in non-line-of-sight environment is a significant advantage of the RFID technology over the conventional bar code systems which can only operate in line-of-sight environment [1]. Nowadays, most of the RFID systems work at four frequency bands: LF (125-134 kHz), HF (13.56 MHz), UHF (860-960 MHz) and microwave frequency (2.4 GHz and 5.8 GHz) bands. Among these frequency bands, UHF band is good at relatively wide reading range and high data-rate. The reading performance of RFID systems are sometimes degraded due to the effect of mutual coupling with surrounding scatterers [2], [3]. In order to solve this problem, near-field RFID system in UHF band has received broad attention [4] in the applications of item-level management such as so-called smart shelf system or conveyor

system, where the RFID tags only in the vicinity of the reader antenna are detected [4]–[6].

Various reader antennas for UHF near-field RFID systems have been reported. In [7], a reader antenna based on the leaky wave microstrip line has been proposed. The detectable region can be controlled by changing the geometry of the microstrip line and the ground plane. The major disadvantage of the reading antenna was the low power efficiency due to the power absorption at the termination load of the leaky wave microstrip line. Therefore, relatively high power supplied to the reader antenna is required in order to activate IC chips embedded in RFID tags. In [8] and [9], array antennas focusing the near-field to a specific region were proposed. Detectable region of the array antennas can be switched flexibly, however, a complicated system composed of microwave components is required to switch the array antennas.

A planar waveguide antenna having leaky waveguide structure consisting of two conducting plates was developed [10]. Upper plate is a mesh plate while bottom one is a solid ground plane and they work as the parallel plate waveguide. The planar waveguide antenna transmits RF power to the RFID tags using evanescent wave on the mesh plate [11]. Detectable area of the planar waveguide antenna is limited to the area on the mesh plate because evanescent wave is localized only on the mesh plate. One of the problems of the planar waveguide antennas is how to alleviate the effect of standing wave, which yields null lines in the detectable region. Termination of the planar waveguide antenna with a matched load is one of the solutions, but it causes power loss at the terminated load [12]. In [13], multiple input ports were introduced to a planar waveguide in order to control its near-field distribution. The effect of the standing wave can be alleviated but the reader antenna becomes complicated and expensive.

In our previous works, switching diversity technique was introduced to the planar waveguide antenna in order to switch the position of the null lines of standing wave parallel to the transverse direction [14]. The planar waveguide antenna is terminated by biased PIN diodes and the positions of the null lines are switched electrically. By switching terminal condition, the detectability can be improved without much power loss at the termination because the planar waveguide antenna is terminated by PIN diodes rather than the matched loads. When the width of planar waveguide antenna is less than a quarter wavelength, there is only the standing wave

Manuscript received May 27, 2020; revised September 10, 2020 and October 30, 2020; accepted November 3, 2020. Date of publication November 23, 2020; date of current version February 20, 2021. (Corresponding author: Kunio Sawaya.)

Yusuke Ozawa, Qiang Chen, and Kunio Sawaya are with the Department of Communications Engineering, Graduate School of Engineering, Tohoku University, Sendai 980-8579, Japan (e-mail: sawaya@ecei.tohoku.ac.jp).

Machiko Oouchida and Masatomo Tokieda are with the Smart Sensing Business Development Project, Teijin Limited, Tokyo 100-8585, Japan.

Digital Object Identifier 10.1109/JRFID.2020.3039016

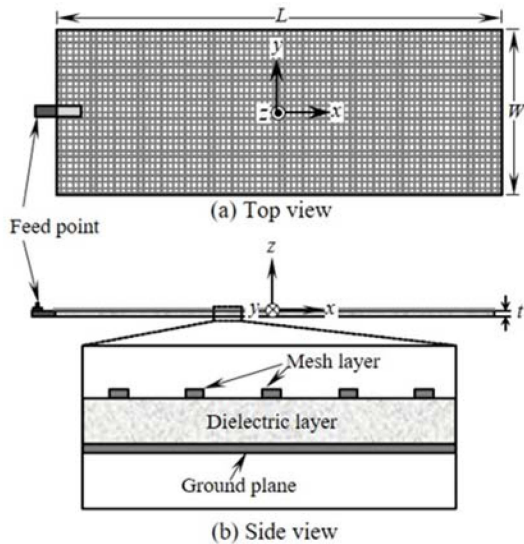


Fig. 1. Geometry of conventional planar waveguide antenna.

along the longitudinal direction and the field distribution along transverse direction is almost uniform.

In this article, a wide planar waveguide antenna for reader of UHF near-field RFID system is proposed, where there are standing waves not only along the longitudinal direction but also along the transverse direction. A pair of notches placed on the planar waveguide antenna is proposed in order to suppress the standing wave current along the transverse direction. In addition, the switching diversity technique is introduced to the proposed planar waveguide antenna which yields robust detectability. Numerical simulation and experiment demonstrate the high detectability of the proposed antenna over conventional one. Finally, a prototype of the proposed planar waveguide antenna for a smart book shelf system is developed to demonstrate the advantage of the proposed planar waveguide antenna with diversity operation.

## II. PRINCIPLE OF PLANAR WAVEGUIDE ANTENNA

Figure 1 shows the geometry of conventional planar waveguide antenna provided by Teijin Limited [10]. This antenna consists of three layers: a conducting mesh layer, a dielectric layer and a solid ground plane. Aluminum is used for the mesh layer and the ground plane. Relative permittivity of the dielectric layer is  $\epsilon_r = 1.3$ . The antenna size is 800 mm in length, 326 mm in width and 2 mm in thickness. The operating frequency is 920 MHz, and thus the width is about one-wavelength. A part of the electromagnetic wave propagating between the mesh layer and the ground plane leaks from the mesh apertures and attenuates exponentially as a function of the distance  $z$  from the surface of the antenna. The rate of the decay of the electric field can be controlled by the size of the mesh apertures [9].

In order to show the basic characteristics of the planar waveguide antenna and confirm the validity of the proposed antenna, numerical simulation using the method of moments (MoM) was performed. Since relative permittivity  $\epsilon_r$  is close to unity and the MoM analysis including the

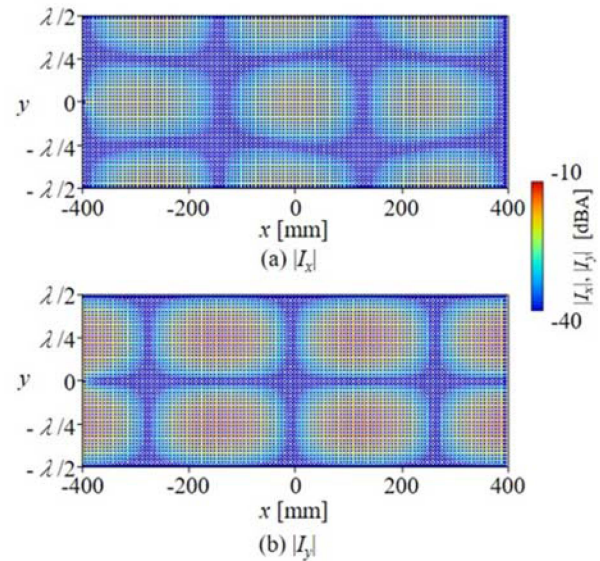


Fig. 2. Simulated current distribution on the mesh layer of conventional planar waveguide antenna.

effect of dielectric substrate requires time-consuming numerical calculation, the dielectric layer is approximately modeled as vacuum.

Figure 2 shows the current distribution on the mesh layer obtained by the MoM analysis. Input power, which is the difference between the incident power and the reflected power, is fixed to be 30 dBm in the simulation of the present paper. It is shown that the current flows along not only longitudinal  $x$  direction but also transverse  $y$  direction of the antenna because the width of the antenna is about one wavelength. Therefore, the near-field null lines occur parallel to both  $x$  direction and  $y$  direction above the antenna.

## III. DESIGN AND SIMULATION OF PROPOSED ANTENNA

### A. Antenna Geometry

Figure 3 shows the proposed antenna geometry schematically. A pair of notches is placed on the mesh layer in order to suppress the transverse current component. The open and short circuits obtained by switches shown in Figure 3 are used to move the position of null lines parallel to transverse  $y$  direction and suppress the effect of the standing wave along longitudinal  $x$  direction [10].

### B. Numerical Simulation

The performance of the proposed waveguide antenna was evaluated by numerical simulation. Figure 4 shows the current distribution on the mesh layer of the antenna with open terminal. The notch position  $d_s$  is set to be 110 mm where the magnitude of current  $|I_y|$  flowing along the edge of the feeding side ( $x = -400$  mm) is maximum. The length of the notch  $L_s$  is selected to be one-quarter of wavelength ( $= 81.5$  mm) to suppress the transverse electric current  $I_y$  along the edge. It is noted that the magnitude of the transverse component of the current  $|I_y|$  is suppressed by the presence of notches except for the region of small  $x$  as shown in Figure 4 (b). It is also

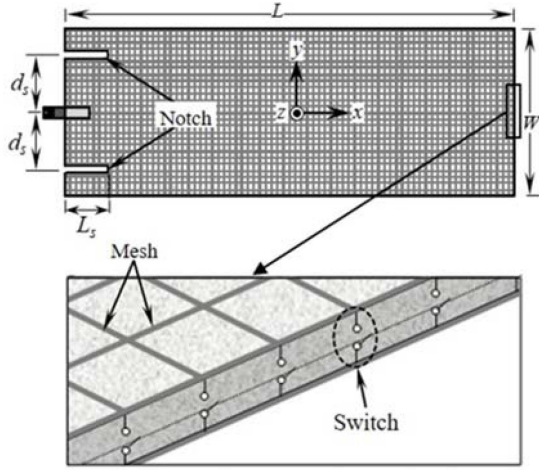


Fig. 3. Geometry of proposed planar waveguide antenna.

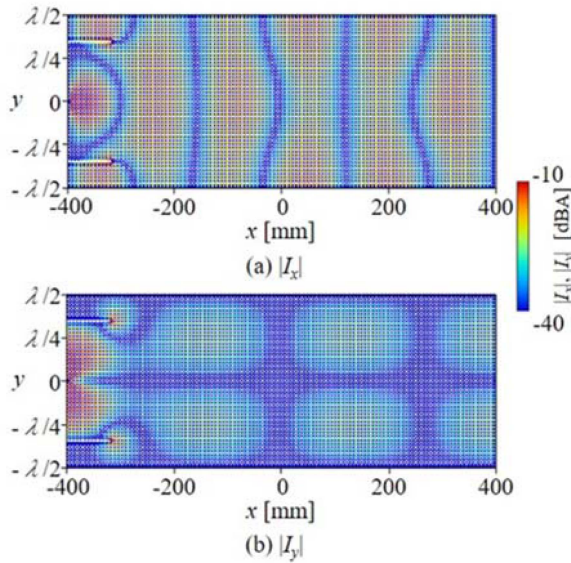


Fig. 4. Current distribution on mesh layer of proposed antenna with open terminal ( $d_s = 110$  mm).

noted that the period of the standing wave along  $x$  decreases as can be seen by comparison with the field distribution in Figure 2. By these observations, it is found that the direction of propagation of the electromagnetic wave traveling between the mesh layer and the ground plane significantly changes by the presence of the notches.

The effect of the notch position  $d_s$  on the current distribution was simulated and the results are shown in Figure 5, where the position of the notch  $d_s$  varies from 110 mm to 125 mm. It is shown that there is little change in the  $x$ -component of current even when the notch position  $d_s$  changes. On the other hand, the  $y$ -component of the current reduces by 32 dB in the case of  $d_s = 120$  mm. Figure 6 shows the distribution of  $z$  component of electric field with open terminal when the notch position  $d_s$  is 120 mm. It can be seen that the near-field null lines parallel to  $x$  direction are eliminated except for the region of small  $x$ .

Next, the effect of switching diversity was evaluated. Figure 7 shows the distribution of  $z$  component of electric

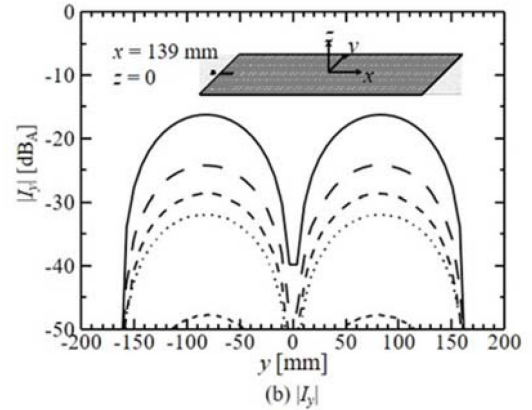
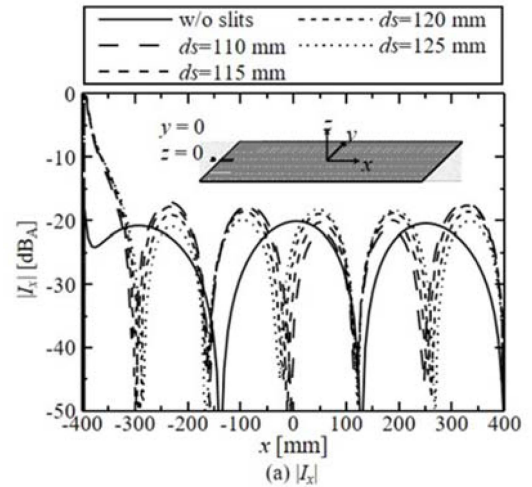


Fig. 5. Simulated current distribution on mesh layer of proposed antenna with varying the position of notch  $d_s$ .

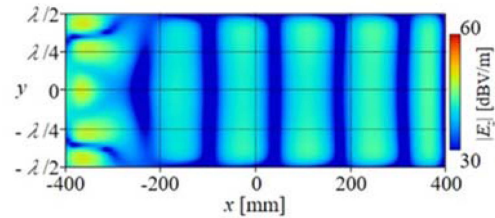


Fig. 6. Simulated distribution of  $|E_z|$  in the horizontal plane ( $z = 30$  mm) of the proposed antenna with open terminal.

field on the antenna with notches when the terminal condition are open and short circuits. It can be seen that the standing wave occurring along longitudinal  $x$  direction varies depending on the terminal condition. Therefore, the standing wave effect along longitudinal direction can be reduced by the diversity operation.

Finally, the electric field distribution in the horizontal plane for the case of the conventional antenna shown in Figure 1 is compared with that of the proposed antenna shown in Fig. 3 having notches with the diversity operation. Figure 8 shows the cumulative distribution function (CDF) of the strength of  $z$  component of electric field, where CDF is defined by the probability that the field strength  $|E_z|$  (V/m) is less than or equal to abscissa. In the case of discrete data,



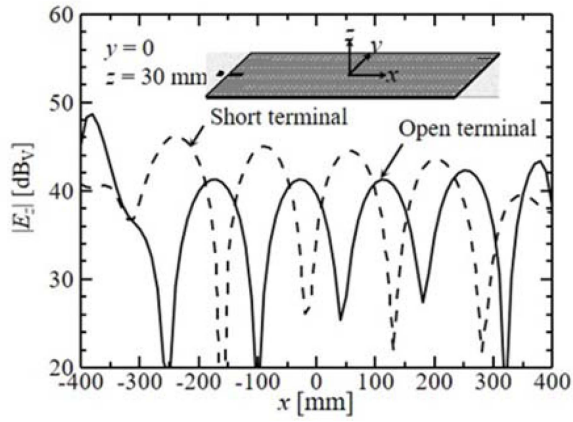


Fig. 7. Simulated distribution of  $|E_z|$  along  $y = 0$  and  $z = 30$  mm with varying terminal condition.

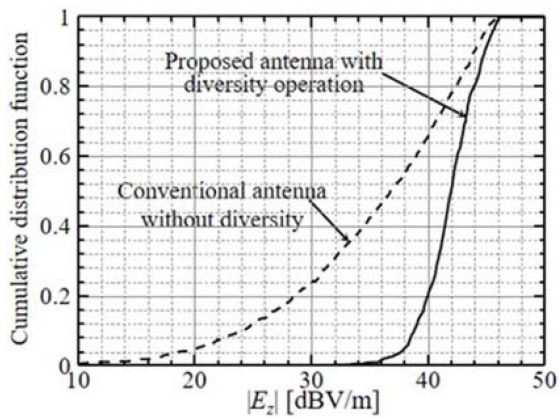


Fig. 8. Cumulative distribution function of  $|E_z|$ .

CDF is the ratio of the number of measured points that the field strength is less than or equal to the value of abscissa divided by the total number of measured data. When the curve moves to right, field strength increases, and when the curve becomes steeper, the distribution of the field strength comes close to more uniform distribution. In Figure 8, the electric field in the vicinity of the feeding point is excluded considering the practical use of the planar antenna. It is found that the CDF of the proposed antenna has steeper curve, which means that the electric field distribution is more uniform than the case of the conventional antenna.

#### IV. EXPERIMENTAL INVESTIGATION

The effect of the notches and switching diversity technique was investigated experimentally. Received power distribution on the planar waveguide antenna was measured by using receiving dipole antenna. Figure 9 shows the measurement system composed of a signal generator (Agilent E4438C), a spectrum analyzer (ROHDE/SCHWARZ FSU-26), dc power supply (KENWOOD PW-36) for the bias of diodes and 3-axis scanner. Figure 10 shows a photo of experimental setup. Conducting plane was inserted to form a parallel plate waveguide in the vicinity of terminal region and switching diodes were inserted at the terminal of the parallel plate waveguide as

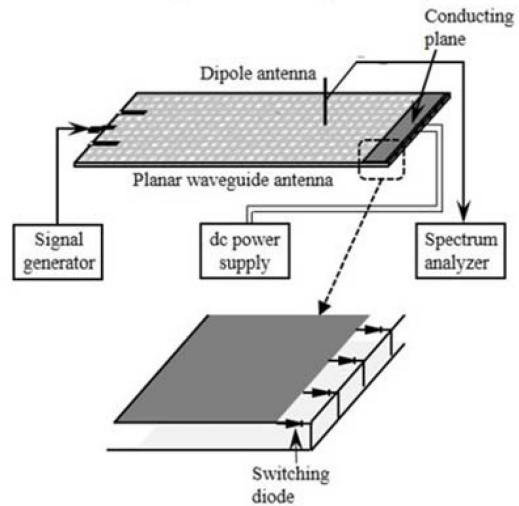


Fig. 9. Experimental setup of near-field measurement.

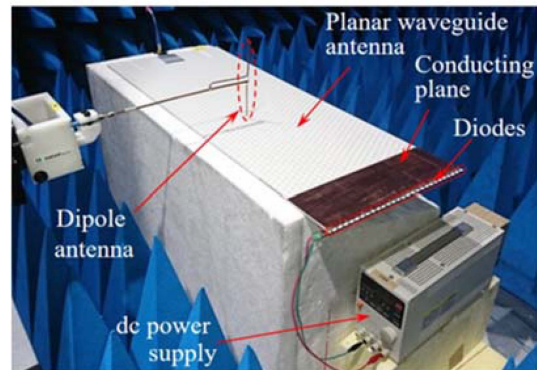


Fig. 10. Photo of experimental setup of near-field measurement.

shown in Figure 9. The switching diodes used in this experiment are Toshiba 1SS352 and the number of diodes is 30. The distance between the lower end of the dipole antenna and planar waveguide antenna is set to be 5 mm. The planar waveguide antenna is made by Teijin Limited and the size of the antenna is almost the same to the numerical analysis model. The notches are placed on the mesh layer and the length of notch  $L_s$  is 77 mm. The notch position  $d_s$  is 90 mm. The parameters of the measurement is listed in Table I. The values of  $L_s$  and  $d_s$  in the experimental investigation are selected to be slightly smaller than those in the numerical investigation in Section III, where the relative permittivity is assumed to be  $\epsilon_r = 1$ .

Figures 11 (a) and (b) show the measured power distribution with varying the bias voltage of diodes in the switching terminal. It can be seen that the standing wave occurring along  $y$  direction is suppressed by the notches. It is also noted that the position of standing wave along longitudinal direction  $x$  moves by changing the value of the bias voltage. Figure 11 (c) shows the received power distribution when the switching diversity operation is employed, where the larger value of the power of Figures 11 (a) and (b) is plotted. It is shown that the near-field nulls parallel to longitudinal direction and transverse direction are almost removed. CDF of the received power distribution is

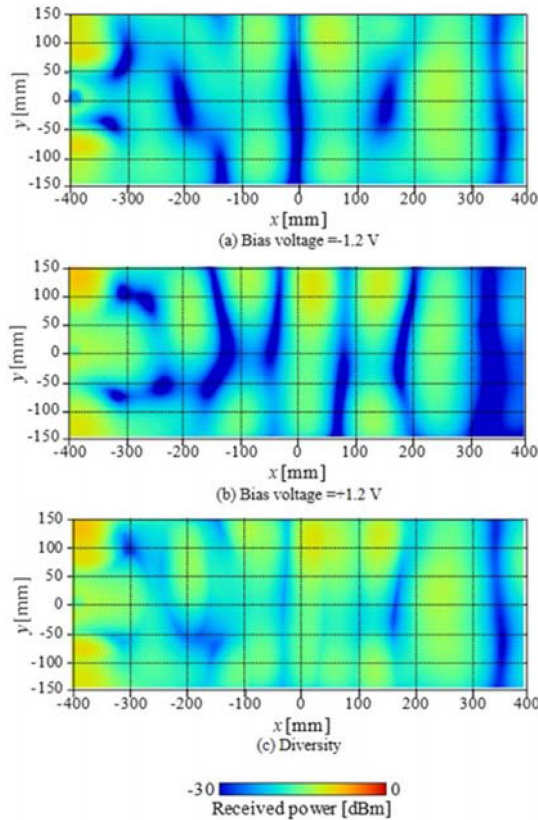


Fig. 11. Received power distribution in horizontal plane of proposed antenna with different bias voltage of diodes in switching operation.

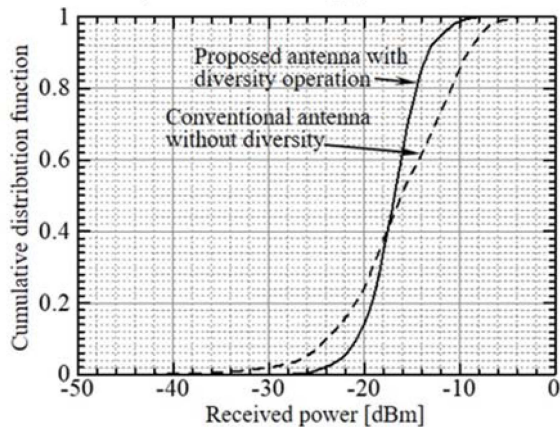


Fig. 12. Cumulative distribution function of received power.

shown in Figure 12, where the received power in the vicinity of the feeding point and switching terminal is excluded. In this case, CDF is defined by the probability that the received power ( $W$ ) is less than or equal to abscissa. By comparison of CDF between the cases of the conventional antenna and proposed antenna with diversity operation, it is noted that CDF of proposed antenna has steeper slope and it is concluded that the received power distribution approaches uniform by placing the notches and introducing the switching diversity.

In the following experiment, bias voltages of  $-1.2$  V and  $1.2$  V were made by a pulse generator. The pulse of

TABLE I  
PARAMETERS OF NEAR-FIELD MEASUREMENT

Frequency	920 MHz
Incident power	15 dBm
Bias voltage	$-1.2$ V, $+1.2$ V

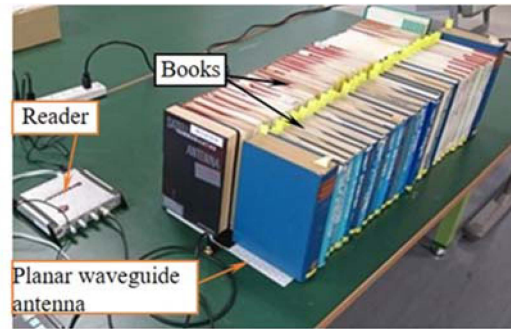


Fig. 13. Experimental setup for measurement setup of RFID tag reading.

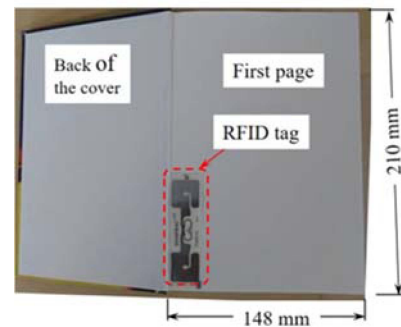


Fig. 14. RFID tag attached on first page.

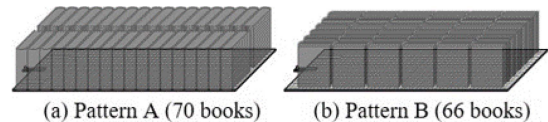


Fig. 15. Arrangement of books and tags.

the 2 voltage levels had the same time duration, and the duty ratio was 0.5. The period of pulse of the bias voltages was decided by the experimental investigation, where an UHF reader/writer [15] and three types of RFID tags were used for the test. These RFID tags were UL-21 [16], DogBone [17] and UhFINE [18]. The experimental results showed that a period longer than 110 ms is required for the desirable diversity effect.

Finally, experimental investigation using practical RFID tags attached to many books in smart-shelf system was performed in order to investigate the advantage of the proposed planar waveguide antenna with diversity operation. Measurement setup is illustrated in Figure 13. The UHF reader/writer and three types of tags are the same to those described above. RFID tag was attached at lower left of the first page of each book as shown in Figure 14. The length between the lower end of tag and the lower edge of the page was 5 mm. A styrofoam sheet with a thickness of

TABLE II  
PARAMETERS OF TAG READING MEASUREMENT

Center frequency	920.4 MHz
Incident power	24 dBm
Bias voltage	-1.2 V, +1.2 V

TABLE III  
MEASUREMENT RESULTS OF READING RATE

	Pattern A	Pattern B
Conventional antenna	67.1 %	73.9 %
Proposed antenna with diversity	95.6 %	93.9 %

5 mm was inserted on the planar antenna and the books with the RFID tag were placed on the styrofoam as shown in Figures 15 (a) and 15 (b). Parameters of the measurement is shown in Table II. Bias voltage of diodes was periodical square wave at 2 Hz to accomplish the switching operation. The measurement was repeated ten times and the average reading rate of the RFID tags was evaluated.

Results of the measurement are shown in Table III. The reading rate of the proposed antenna achieves over 93% for both pattern A and pattern B, which is larger than the case of conventional antenna. The reading rate is defined by the ratio of the number of read tags for one reading cycle divided by the total number of tags. Since there was a small randomness of electromagnetic field, the reading rate slightly changed depending on the reading cycle, averaged reading rate over 10 cycles is shown Table III. The number of tags which cannot be read at all decreases by repeating the reading cycle. In many actual circumstances, all tags can be read by repeating several cycles when the reading rate is greater than 90%.

The detection performance of the RFID tags attached to books depends on the height of tags and it deteriorates as the height increases. It also depends on the strength of multiple scattering waves produced by the surrounding objects. The height of the lower end of tag measured from the upper surface of planar waveguide antenna is usually about 1 cm and desirable detection performance can be obtained. The received voltage of the tag decreases as the height increases, however, detection performance is favorable even when the height is 10 cm, provided the multiple scattering waves are significantly weak.

### V. CONCLUSION

In this article, UHF near-field RFID reader antenna based on leaky waveguide has been proposed and its performance was evaluated using numerical simulation and experiment. In order to suppress the standing wave on the antenna along transverse direction, a pair of notches was placed on the transverse edge of the mesh layer of the planar waveguide. Diversity operation by switching impedance of the terminal load of the planar waveguide antenna was introduced to suppress the standing wave effect along longitudinal direction.

It has been shown by numerical simulation and experiment that the near-field nulls along the transverse direction

is almost removed by the presence of the notches of the proposed antenna and the distribution of the field strength becomes almost uniform by the use of the switching diversity. Moreover, it has been demonstrated that the reading performance of the commercial RFID tags attached to many books for the proposed antenna with diversity is greatly improved by comparison with that of the conventional antenna.

Employment of the proposed methods in the reader antennas of practical RFID system may yield an indispensable increase of the manufacturing costs, but the cost is acceptable when considering the significant improvement in reading performance of the RFID system obtained by the proposed methods.

### REFERENCES

- [1] K. Finkenzeller, *RFID Handbook*. Hoboken, NJ, USA: Wiley, 2010.
- [2] P. V. Nikitin and K. V. S. Rao, "Performance limitations of passive UHF RFID systems," in *Proc. IEEE Antennas Propag. Soc. Int. Symp.*, Oct. 2006, pp. 1011–1014.
- [3] D. M. Dobkin and D. M. Weigand, "Environmental effects on RFID tag antennas," in *Proc. IEEE MTT-S Int. Microw. Symp.*, Jun. 2005, pp. 135–138.
- [4] P. V. Nikitin, K. V. S. Rao, and S. Lazar, "An overview of near field UHF RFID," in *Proc. IEEE Int. Conf. RFID*, Mar. 2007, pp. 167–174.
- [5] J. Shi, X. Qing, Z. N. Chen, and C. K. Goh, "Electrically large dual-loop antenna for UHF near-field RFID reader," *IEEE Trans. Antennas Propag.*, vol. 61, no. 3, pp. 1019–1025, Mar. 2013.
- [6] Y. Yao, Y. Liang, J. Yu, and X. Chen, "Design of a multipolarized RFID reader antenna for UHF near-field applications," *IEEE Trans. Antennas Propag.*, vol. 65, no. 7, pp. 3344–3351, Jul. 2017.
- [7] C. R. Medeiros, J. R. Costa, and C. A. Fernandes, "RFID reader antennas for tag detection in self-confined volumes at UHF," *IEEE Antennas Propag. Mag.*, vol. 53, no. 2, pp. 39–50, Apr. 2011.
- [8] H.-T. Chou, C.-T. Yu, K.-T. Wang, and P. Nepa, "A simple design of patch antenna array with an optimized field distribution in the near-zone for RFID applications," *IEEE Antennas Wireless Propag. Lett.*, vol. 13, pp. 257–260, Feb. 2014.
- [9] W. Choi, J. S. Kim, G. Choi, and J. S. Chae, "Near-field antenna for RFID smart shelf in UHF," in *Proc. IEEE Antennas Propag. Soc. Int. Symp. USNC/URSI Nat. Radio Sci. Meeting (APSURSI)*, Jun. 2009, pp. 1280–1283.
- [10] *Teijin Limited*. Accessed: Mar. 7, 2014. [Online]. Available: [https://www.teijin.com/news/2014/ebd140307\\_11.html](https://www.teijin.com/news/2014/ebd140307_11.html)
- [11] H. Shinoda, Y. Makino, N. Yamahira, and H. Itai, "Surface sensor network using inductive signal transmission layer," in *Proc. Int. Conf. Netw. Sensing Syst. (INSS)*, Jun. 2007, pp. 201–206.
- [12] A. O. Lim, K. Tezuka, and B. Zhang, "An experiment study of electromagnetic field distribution over 2D communication system," in *Proc. Asia Pac. Microw. Conf. (APMC)*, Dec. 2009, pp. 1266–1269.
- [13] T. Kagawa, T. Matsuda, B. Zhang, and Y. Kado, "Power provision scheme considering shadowing effect for two-dimensional communication systems," in *Proc. Asia Pac. Conf. Commun. (APCC)*, Aug. 2013, pp. 525–530.
- [14] K. H. Chen, Q. Chen, K. Sawaya, M. Oouchida, and Y. Hirano, "Diversity reception of 920 MHz RFID reader antenna in smart-shelf system," in *Proc. Int. Symp. Antennas Propag. (ISAP)*, Nov. 2015, pp. 851–853.
- [15] *Speedway Revolution R420*, Impinj, Inc., Seattle, WA, USA. Accessed: Nov. 2017. [Online]. Available: <https://www.impinj.com/platform/connectivity/speedway-r420/>
- [16] *UL-21*, Dai Nippon Printing Company, Ltd., Shinjuku, Japan. Accessed: Nov. 2017. [Online]. Available: [http://www.dnp.co.jp/infosol/solution/detail/10097539\\_18793.html](http://www.dnp.co.jp/infosol/solution/detail/10097539_18793.html)
- [17] *DogBone*, SMARTRAC N. V., Amsterdam, The Netherlands. Accessed: Nov. 2017. [Online]. Available: <https://www.smartrac-group.com/dogbone.html>
- [18] *UhfINE (HDCN-9522)*, Wizard, Inc., Shibuya, Japan. Accessed: Nov. 2017. [Online]. Available: <http://www.ezipsec.com/wp-content/uploads/2015/09/20111101.pdf>





**Yusuke Ozawa** received the Graduation degree from the Faculty of Engineering, Tohoku University, Sendai, Japan, in 2016, and the M.E. degree in the subject of communications engineering from Graduate School, Tohoku University in 2018. During his M.E. study, he performed research on the UHF RFID reader antenna.



**Machiko Oouchida** received the B.E. and M.E. degrees from Hiroshima University, Higashi-Hiroshima, Japan, in 2004 and 2006, respectively. She joined Teijin Limited, where she is currently with Technology Development Team, the Smart Sensing Business Development Project.



**Qiang Chen** (Senior Member, IEEE) received the B.E. degree from Xidian University, Xi'an, China, in 1986, and the M.E. and D.E. degrees from Tohoku University, Sendai, Japan, in 1991 and 1994, respectively, where he is currently a Chair Professor of Electromagnetic Engineering Laboratory with the Department of Communications Engineering, Faculty of Engineering. His primary research interests include antennas, microwave and millimeter wave, electromagnetic measurement, and computational electromagnetics. He received the

Best Paper Award and the Zen-ichi Kiyasu Award in 2009, from the Institute of Electronics, Information and Communication Engineers (IEICE). He served as the Chair of IEICE Technical Committee on Photonics-Applied Electromagnetic Measurement from 2012 to 2014, the Chair of IEICE Technical Committee on Wireless Power Transfer from 2016 to 2018, and the Chair of IEEE Antennas and Propagation Society Japan Chapter from 2017 to 2018. He is currently the Chair of IEICE Technical Committee on Antennas and Propagation, and a Fellow of IEICE.



**Kunio Sawaya** (Life Fellow, IEEE) received the B.E., M.E., and Ph.D. degrees from Tohoku University, Sendai, Japan, in 1971, 1973, and 1976, respectively, where he was a Research Associate, an Associate Professor, and a Professor with the Department of Electrical and Communication Engineering from 1976 to 2013. He is a Professor Emeritus with Tohoku University. He was also a Specially Appointed Professor of the Promotion Office with Strategic Innovation, Tohoku University from 2015 to 2019. His areas of interests are anten-

nas in plasma, antennas for mobile communications, theory of scattering and diffraction, antennas for plasma heating, and array antennas. He received the Paper Awards in 1988 and 2009, the Communications Society Paper Awards in 2006 and 2014, and the Zen-ichi Kiyasu Award in 2009 all from the Institute of Electronics, Information and Communication Engineers (IEICE). He served as the Chair of the Technical Group with Antennas and Propagation of IEICE from 2001 to 2003, the Chair of the Organizing and Steering Committees of 2004 International Symposium on Antennas and Propagation (ISAP'04), the President of the Communications Society of IEICE from 2009 to 2010, and the Chair of IEEE Sendai Section from 2012 to 2013. He is a Fellow and an Honorary Member of IEICE.



**Masatomo Tokieda** received the B.E. degree from Oita University in 1995, and the M.E. degree from Kumamoto University, Kumamoto, Japan, in 1997. In 2016, he joined Teijin Limited, where he is currently a Product Manager with the Smart Sensing Business Development Project.